

## Turbulence Structure of the Convective Boundary Layer. Part II: Phoenix 78 Aircraft Observations of Thermals and Their Environment

GEORGE S. YOUNG\*

*Department of Meteorology, The Pennsylvania State University, University Park, Pennsylvania*

(Manuscript received 15 January 1987, in final form 4 September 1987)

### ABSTRACT

A conditional sampling technique based upon the mixed layer spectra of vertical velocity and temperature is developed. This technique is used to analyze the turbulence data obtained by aircraft during the Phoenix 78 convective boundary layer experiment. Observations of the size, spacing and structure of thermals as well as their contribution to mixed layer processes are presented. Implications of these results for pollution dispersion are discussed. The observed scale dependence is also used to estimate what fraction of a turbulence statistic must be accounted for by the subgrid parameterizations of large eddy simulations.

### 1. Introduction

Thermals are buoyantly driven convective eddies which generate most of the turbulence in the unstable atmospheric boundary layer. These eddies are composed of thermal updrafts and their compensating environmental downdrafts, both of which span the depth of the convective boundary layer (CBL) (Taconet and Weill, 1983). The horizontal scales of thermal circulations range around 1.5 times the CBL depth,  $z_i$  (Caughey and Palmer, 1979). Thermals are both a result of and the primary controlling mechanism for the mean CBL stability profile (Lenschow and Stephens, 1982; Wyngaard and Brost, 1984). The earth's surface is the buoyancy source for the CBL, providing heat and/or moisture to its lower boundary (Deardorff, 1970; Kaimal et al., 1976; Lenschow and Stephens, 1980). The structure and dynamics of the eddies which arise from this addition of buoyancy are important controlling factors for diffusion within the CBL (Lamb, 1978). Furthermore, these thermal circulations help drive entrainment across the capping inversion (Caughey and Palmer, 1979; Rayment and Readings, 1974).

A conditional sampling technique is needed to distinguish thermals from their environment in a turbulence data series. By conditional sampling, the turbulence in thermal updrafts and environmental downdrafts can be studied and compared. A review of the

literature shows just how sensitive the quantitative results are to the criteria used to distinguish thermals from their environment. Therefore, the use of a physically meaningful set of criteria is essential if the statistics computed from the conditional samples are to have maximum usefulness.

### 2. Procedures

#### a. Data collection

The turbulence data were collected by NCAR Queen Air aircraft during the September 1978 Phoenix CBL experiment at the Boulder Atmospheric Observatory (BAO). The 58 horizontal flight legs, each approximately 35 km long, were distributed approximately evenly from  $0.1z_i$  to  $1.3z_i$ . The ratio of boundary layer depth to the Monin-Obukhov length ranged from  $-11$  to  $-164$ , indicating the dominance of buoyant convection over shear-produced turbulence over this height range. Further information on the BAO site, weather conditions, observational equipment, data collection and filtering is contained in Part I (Young, 1988).

#### b. Distinguishing thermals from their environment

##### 1) CONDITIONAL SAMPLING METHODS OF PREVIOUS STUDIES

A number of conditional sampling methods have been used in the past to distinguish thermals from their environment. Each of these methods is derived from a particular definition of the term thermal. Several conflicting definitions are in use. Scorer and Ludlam (1953) define thermals as buoyant parcels of fluid while Taconet and Weill (1983) and Greenhut and Khalsa (1982) define thermals as convective updrafts. These updrafts are generally coherent throughout the depth

\* The bulk of this research was conducted at the Department of Atmospheric Science, Colorado State University.

Corresponding author address: Dr. George S. Young, Department of Meteorology, Pennsylvania State University, 503 Walker Building, University Park, PA 16802.

of the CBL. Grossman (1984) shows that these two definitions are contradictory. In the upper CBL, the updrafts are negatively buoyant on the average. Also, the updrafts contain entrained parcels of environmental air which have buoyancies opposite that of the rest of the updraft at that level. Thus, a definition of thermals based on positive buoyancy will include downward moving air of free atmospheric origin while excluding upward moving air of environmental origin. Similarly, Grossman (1984) shows through bivariate conditional sampling that a tracer of surface origin does not unambiguously define a convective updraft because of horizontal mixing between updrafts and downdrafts. Thus, a conditional sampling criteria based on vertical velocity is necessary for application of the convective updraft definition of thermals.

The choice of a  $w$  threshold and a minimum width controls the differentiation of thermals from regions of mesoscale ascent and from small-scale fluctuations on thermals. Greenhut and Khalsa (1982) and Khalsa and Greenhut (1985a) used different  $w$  thresholds to distinguish updrafts and downdrafts from their environment. These thresholds were related to  $w$  variances so that they automatically adjusted for varying levels of turbulence. A minimum thermal size of 40 m was used.

## 2) CONDITIONAL SAMPLING METHODS OF THE CURRENT STUDY

The technique for distinguishing thermals in the present study is also based on identification of  $w$  perturbation events. Determination of physically meaningful minimum and maximum horizontal scales for thermal circulations is based on the Phoenix 78 vertical velocity and temperature spectra presented in Young (1987). The spectra can be divided into three wavelength ranges, mesoscale subrange, buoyant production subrange and inertial subrange.

It is desirable to separate the quasi two-dimensional mesoscale motions from the three-dimensional convective eddies because they are generated by very different mechanisms. High pass filtering with a cutoff wavelength of  $10z_i$  eliminates most of the mesoscale contribution to the data series while leaving most of the convective contribution intact as discussed in Part I and Young (1987). This cutoff wavelength lies in or near the spectral gap for temperature and at 6.6 times the dominant wavelength for  $w$ . This cutoff wavelength is less than a third of the flight leg length so trends are adequately removed. Previous studies have used a variety of techniques involving detrending and nonzero thresholds for this purpose.

Inertial subrange turbulence is dynamically different from boundary layer convection in that it receives its energy by inertial cascade from larger scales rather than by buoyant production or vertical transport. The inertial subrange contribution was removed from the  $w$  series used to define thermals by low pass filtering with a cutoff wavelength of  $0.1z_i$ . This cutoff wavelength

was somewhat arbitrarily chosen to ensure that only those scales at which the  $w$  and temperature spectral slopes were characteristic of inertial cascade were filtered out. A variety of minimum event width criteria have been used in previous studies for this purpose. The 40 m minimum event width used by Greenhut and Khalsa (1982) and Khalsa and Greenhut (1985a) is roughly equivalent to the  $0.1z_i$  wavelength cutoff given their average boundary layer depth of 680 m.

Those parts of the data series with filtered vertical velocities greater than zero were defined as thermal updrafts while the remainder were classified as environmental downdrafts. This is not as restrictive a definition as that of Greenhut and Khalsa (1982) and Khalsa and Greenhut (1985a) which included a positive  $w$  threshold.

## 3. Observations

### a. Fractional area coverage, width and spacing of thermals

The fractional area coverage by thermals is shown in Fig. 1 as a smooth profile was drawn to fit the 58 measured values. The fractional coverage decreases from approximately 0.50 at the surface to a minimum of less than 0.43 in the mid-CBL and increases again to approximately 0.50 at and above  $z_i$ .

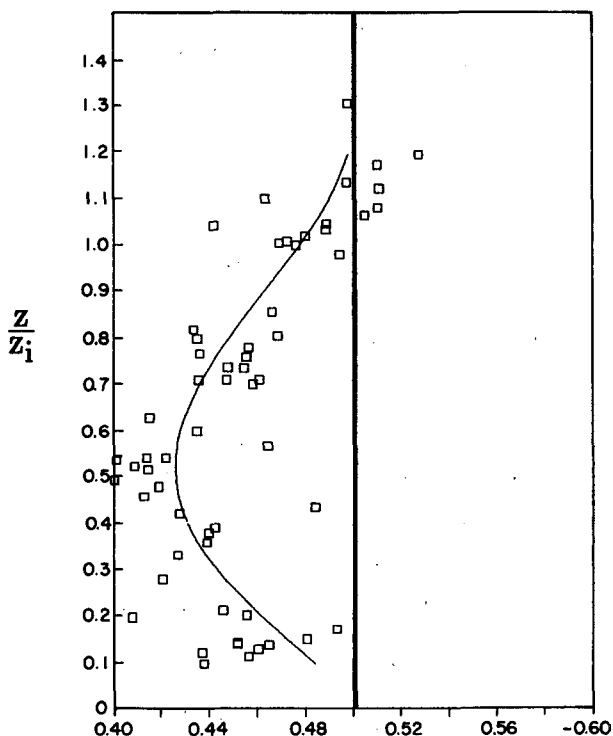


FIG. 1. The vertical profile of the fraction of the area covered by thermals. The vertical scale is the height divided by the depth of the convective boundary layer.

The fractional area coverage by thermals can be approximated by

$$\sigma = 0.5 - 0.35 \left( \frac{z}{z_i} \right)^{3/2} \left( 1.3 - \frac{z}{z_i} \right)^{9/4}$$

where  $\sigma$  is the fractional area coverage by thermals,  $z$  is the height and  $z_i$  is the height of the inversion base.

Previous observational studies have yielded a variety of values for the fractional area coverage by thermals. Manton (1977) reported a value of 0.42 for the lower CBL. Coulman (1978) observed values ranging from 0.36 to 0.42 with a minimum at intermediate levels in the CBL. Lenschow and Stephens (1982) give the value as 0.28 for the entire depth of the Airmass Transformation Experiment (AMTEX) CBL. Greenhut and Khalsa (1982) computed 0.16 coverage by updrafts, 0.24 coverage by downdrafts and designated the remaining 0.60 as environment. Their observations were taken at  $0.3z_i$  over the central equatorial Pacific Ocean. The two previous studies with the largest fractional area coverage by thermals used temperature thresholds selected such that the expected value of  $w$  at the threshold would be zero. The other studies used more restrictive thresholds and so obtained smaller values.

Lamb (1978) used large eddy simulation (LES) methods to estimate the fractional area coverage by thermals. The limited horizontal resolution of the numerical model acted as a minimum horizontal scale for thermals. The amplitude threshold was zero  $w$ . The fractional area coverage approached 0.50 near the surface and above  $z_i$  with a minimum of about 0.37 near  $0.8z_i$ . This profile is qualitatively similar to that of the present study but with the minimum located higher in the CBL.

Both observational and modelling results confirm that the fractional area coverage by thermals is less than 0.50 throughout most of the CBL. Values approach 0.50 only at the surface and within the capping inversion. Estimates of minimum coverage in the mid CBL range from 0.36 to 0.43 for those studies which used a zero expected vertical velocity threshold. As pointed out by Lamb (1978) this observed minimum has important implications for the diffusion of pollutants in the CBL.

Thermals and the subsiding environmental regions between them come in a variety of widths. The width distribution of thermals can be approximated by the distribution of flight path segments inside thermals (Lenschow and Stephens, 1980). The distribution of thermal updraft widths is shown in Fig. 2a. The observed distribution is approximately lognormal and scales with  $z_i$ . The environmental downdraft width distribution shown in Fig. 2b is similar. Melling and List (1980) also found that updraft and downdraft widths scaled with  $z_i$  and were lognormally distributed. Neither study found any significant variation of these distributions with height within the CBL.

Lopez (1977) showed that convective cloud sizes are lognormally distributed as well. Lopez proposed two mechanisms for the genesis of lognormal distributions for convective element widths. The first mechanism is stochastic growth in which entrainment is a random variate proportional to size of the convective element. The second mechanism is stochastic formation in which merger of small elements leads to the final lognormal distribution. Both of these mechanisms are compatible with what is known of the formation of thermals.

The observed distributions of convective element widths may, however, be an artifact of the limited resolution of any observational method. If the actual distribution of widths were exponential, smoothing during the observational process would result in a distribution which approximates the gamma. The scatter in the current data prohibits distinction between the gamma and the similarly shaped lognormal distribution. The fact that the observed modes of the width distributions were within a factor of two of the cutoff wavelength for both the current study and Melling and List (1980) suggests that the number of small updrafts has been greatly reduced by this smoothing. Therefore, it is possible that the actual updraft and downdraft width distributions are exponential. The value of the observed modes (geometric means for lognormal distributions) are therefore of doubtful significance.

The width of thermal updraft which occupies the largest fraction of the CBL area is  $0.45z_i$ . The width of environmental downdraft which occupies the largest fraction of the CBL is  $0.55z_i$ . The resulting width for updraft/downdraft pairs,  $1.0z_i$ , is fairly consistent with the  $w$  spectra which show a dominant wavelength of approximately  $1.5z_i$  for the bulk of the CBL (Kaimal et al., 1976; Young, 1987). The peaks of the distributions and of the spectra are fairly broad so the uncertainty in these two measures of the CBL length scale is as great as the difference between them.

Arithmetic mean thermal widths for the individual flight legs ranged from  $0.15z_i$  to  $0.35z_i$  with a slight tendency to increase with height. Lenschow and Stephens (1980) and Khalsa and Greenhut (1985a,b) also report increases with height. Melling and List (1980) report a relatively large arithmetic mean thermal width of  $0.52z_i$  suggesting that the relatively coarse horizontal resolution of their sodar had indeed reduced the number of small thermal updrafts detected.

The arithmetic mean number density of thermals ranged from 1.4 to 2.8 for the individual flight legs with no detectable vertical trend. Thus, the average horizontal spacing between thermals is about  $0.5z_i$  whereas the dominant horizontal length scale in the CBL is about  $1.5z_i$ . This implies that thermals cluster or equivalently that small downdrafts often occur in the midst of thermals. Thermals were packed twice as closely in this study as in the AMTEX results of Lenschow and Stephens (1980). The observations of Khalsa

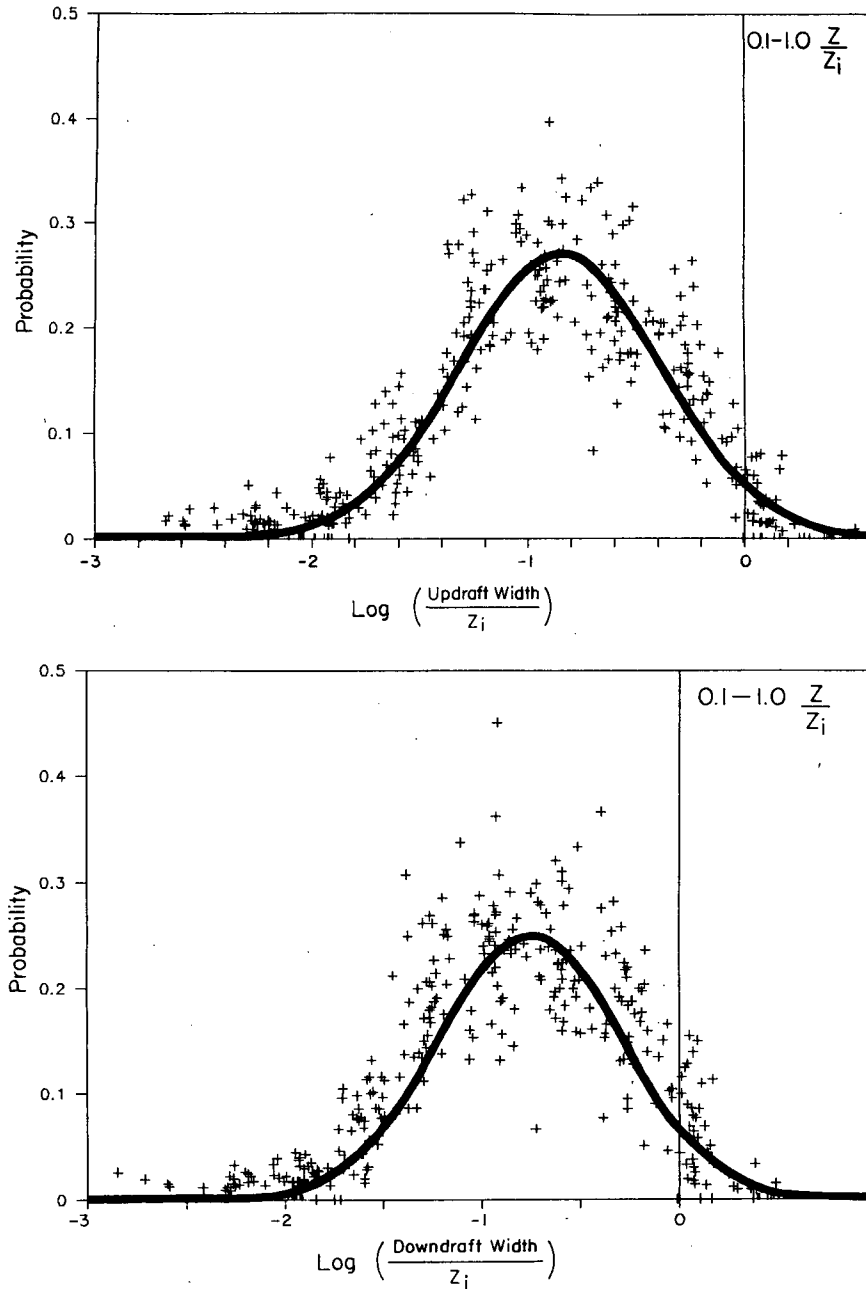


FIG. 2a-b. Normalized histograms of the width of thermal updrafts and environmental downdrafts in the convective boundary layer. The horizontal axis is the logarithm of width divided by the depth of the convective boundary layer. The vertical axis is frequency of occurrence normalized so that the area under the curve equals unity. The observations of the frequency of observation for each size bin are marked as +. The figure includes the data from a number of horizontal flight legs. The solid lines are lognormal distributions plotted for comparison.

and Greenhut (1985a,b) are midway between those of the other two studies.

*b. Plume mean buoyancy and vertical velocity profiles*

Profiles of the mean buoyancy perturbation and mean vertical velocity in thermals and their environ-

ment will be presented in this section. The profiles are nondimensionalized with the mixed layer scaling parameters. The nondimensionalized  $\theta_v$  perturbations are equivalent to nondimensionalized buoyancy. This quantity is the fundamental energy source for the motions of thermals and their environment. The profiles

of buoyancy in thermals and their environment are shown in Fig. 3. The buoyancy of thermals is about 1.0 at  $0.1z_i$  and decreases almost linearly to zero at  $0.65z_i$  and on to approximately  $-0.3$  just below  $z_i$  before tending back to zero above  $z_i$ . This is the pattern expected for buoyantly driven thermals penetrating into layers with greater static stability. The buoyancy profile of the environment is of similar shape and opposite sign as required to achieve zero mean buoyancy at each level.

The buoyancy profiles for thermals and their environment can be approximated by

$$\frac{\overline{\theta_{vT}}}{\theta_*} = -0.5 \left( 1.0 - \frac{0.2}{[1 + 100(0.9 - z/z_i)^2]} \right) + 2 \left| 0.9 - \frac{z}{z_i} \right|$$

and

$$\frac{\overline{\theta_{vE}}}{\theta_*} = \frac{-\sigma \overline{\theta_{vT}}}{1 - \sigma}$$

respectively. The  $\overline{\theta_{vT}}$  and  $\overline{\theta_{vE}}$  are the average virtual temperature perturbations and  $\theta_*$  is the mixed layer virtual temperature scale.

Lenschow and Stephens (1980) present a buoyancy profile for AMTEX thermals which has a value of 3.0 at  $0.1z_i$ , more curvature in the lower and mid CBL and no negative area at all. The addition of buoyancy by convective clouds during AMTEX may explain the lack of a negatively buoyant area. Khalsa and Greenhut (1985a,b) also show a decrease in buoyancy with height.

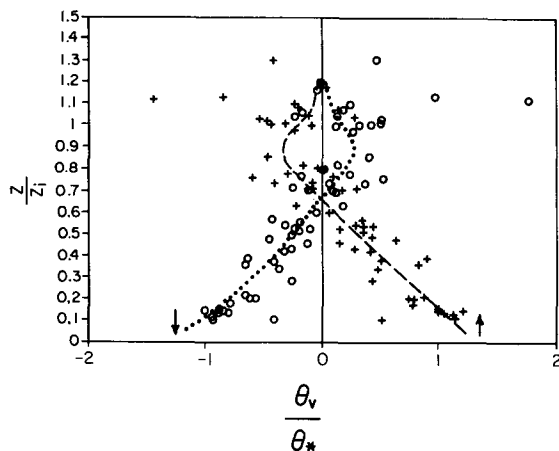


FIG. 3. The vertical profiles of the normalized plume mean virtual potential temperatures. The horizontal scale has been normalized by  $\theta_*$ . The vertical scale is height divided by the depth of the convective boundary layer. The dashed curve is the profile for thermal updrafts and the dotted curve is the profile for environmental downdrafts. The estimates of the plume mean virtual potential temperature from the individual flight legs are plotted as + for thermal updrafts and o for environmental downdrafts.

Their values were similar to those measured in AMTEX. The larger buoyancies reported in these two studies are consistent with the more restrictive definitions of thermals used. Neither of the previous studies which used a zero expected vertical velocity threshold reported normalized buoyancy values. Therefore, the universality of the present result cannot be tested by comparison with past results.

Because  $\theta_*$ , which was used to nondimensionalize the  $\theta_v$  perturbations, is of order  $0.1^\circ\text{C}$ , stabilities of less than  $1^\circ\text{C}$  across the depth of the boundary layer would be sufficient to eliminate thermals. Boundary layers with such stabilities have traditionally been considered well mixed. Such boundary layers are not well mixed from the point of view of the dynamics of thermals. Therefore, because thermals are the dominant mixing eddy in the CBL, a slight change in the mean stability of the boundary layer would have a large effect on the diffusive transports of momentum and scalar contaminants. The extent to which buoyancy flux convergence can adjust to damp out changes in the CBL stability profile has yet to be determined. This feedback loop between the vertical velocity of thermals, the stability of the CBL and the buoyancy flux convergence may be important in determining the degree of diffusion in CBLs with nonzero mean vertical motion or differential  $\theta_v$  advection.

The mean  $w$  in thermals is the primary measure of the strength of the buoyantly driven vertical circulations in the CBL. The profiles of mean  $w$  in thermals and their environment are shown in Fig. 4. The mean  $w$  in thermals increases from zero at the surface to approximately 0.56 at  $0.33z_i$ . The value then decreases to approximately 0.25 at  $z_i$  and on to zero a short distance above that. Because the profile of fractional area coverage by thermals has a minimum in the mid CBL, the maximum magnitude of the mean environmental downdraft is located lower than that for the mean thermal updraft. This extremum is located at  $0.19z_i$  and has a value of  $-0.46$ . Above this level the mean environmental downdraft weakens to  $-0.23$  at  $z_i$  and then on to zero.

The vertical velocity profiles for thermals and their environments can be approximated by

$$\frac{\overline{w_T}}{w_*} = 0.85 \left( \frac{z}{z_i} \right)^{1/3} \left( 1.3 - \frac{z}{z_i} \right)$$

and

$$\frac{\overline{w_E}}{w_*} = \frac{-\sigma \overline{w_T}}{1 - \sigma}$$

respectively. The  $\overline{w_T}$  and  $\overline{w_E}$  are the average vertical velocities and  $w_*$  is the mixed layer vertical velocity scale.

Lenschow and Stephens (1980) found similar profile shapes with the maximum amplitudes decreased and lowered slightly. Khalsa and Greenhut (1985a) report

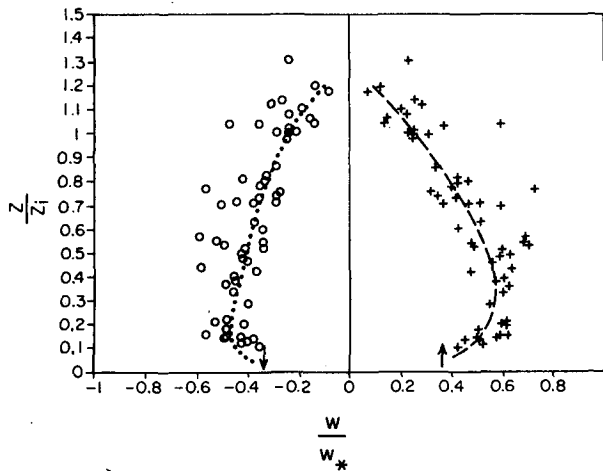


FIG. 4. As in Fig. 3 except for vertical velocity.

mean vertical velocities in thermals of about 1.0 near  $0.2z_i$ . These values are significantly greater than those reported elsewhere because the 60% of the CBL air with the least vertical velocity was not included in the averages for either updrafts or downdrafts. Lamb (1978) used LES techniques to estimate the profile of mean  $w$  in thermals and their environment. The maximum of thermal updraft strength was 0.61 at  $0.3z_i$ , and the maximum of environmental downdraft strength was  $-0.47$  at  $0.2z_i$ . These model derived values are very close to those measured in the CBL during Phoenix 78.

The observed maximum value of the mean vertical velocity in thermals was smaller than the vertical velocity which would be achieved by a parcel freely accelerating to that level under the influence of the observed buoyancy profile. This suggests that the net effect of drag by lateral mixing between thermals and their environment and any pressure forcing is to reduce the rate of acceleration in the lower CBL.

### c. Contribution of thermals to turbulent variance and covariance statistics

Knowledge of the contribution of thermal updrafts and environmental downdrafts to turbulence in the CBL is fundamental to the understanding of the dynamics of the CBL. In addition, the degree to which motions on this scale dominate the turbulence structure of the CBL determines the degree of accuracy needed for the subgrid turbulence parameterizations of an LES. The contributions of these eddies to the variances of  $\theta_v$  and  $w$  as well as to their covariance will be discussed in this section.

There are two ways to measure the contribution of thermal updrafts and environmental downdrafts to these turbulent statistics. First they can be computed from the plume mean quantities presented in the previous section. This type of calculation yields the frac-

tion of the total statistic which is accounted for by the simple two plume conceptual model. This type of model approximates the vertical circulations of the CBL as two flows, one upward and the other downward, each of which is horizontally homogeneous but is permitted to vary in the vertical. This has traditionally been called the top hat model. The top hat model has been popular because of its simplicity. The fraction of a turbulence statistic which can be explained by the top hat model will be called the top hat contribution to that statistic.

The second way of estimating these statistics is to include all of the scales of thermal motion in the calculation, while eliminating the contributions of mesoscale circulations and the inertial subrange as described in the procedures section. This is analogous to computing the resolvable scale turbulence statistics from the results of an LES. The fraction of a turbulence statistic which can be explained by these scales of motion will be referred to as the thermal scale contribution to that statistic.

The turbulence statistic computed from a data series containing both thermal scale and inertial subrange turbulence (that is, a series with only the mesoscale circulations filtered out) will be used as the reference value for the total statistic. The top hat contribution and the thermal scale contribution will be given as fractions of this total.

The top hat contribution and the thermal scale contribution to  $\theta_v$  variance for the individual flight legs are shown in Fig. 5. The thermal scale motions contribute 80% to 95% of the total variance in the low to mid CBL and an even larger fraction at higher levels. This variation with height is a result of variations in the spectra with height. Caughey and Palmer (1979) showed  $\theta$  spectra for the CBL and for the stable air above it. The observed spectral slope at horizontal

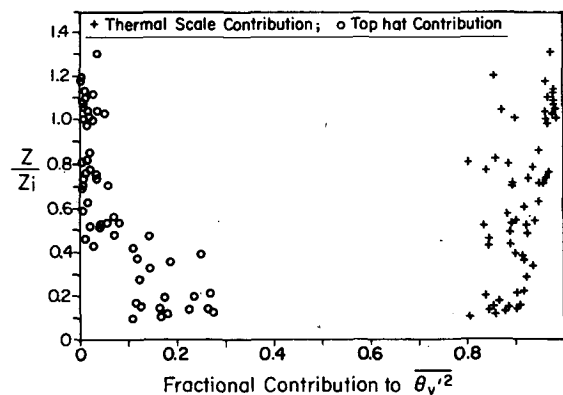


FIG. 5. The fractions of the total virtual potential temperature variance contributed by two scales of motion are shown as functions of height. The vertical axis is height divided by the depth of the boundary layer. Each point represents an individual flight leg. The ratios of the thermal scale contribution to the variance to the total variance are plotted as +. The ratios of the top hat contribution to the variance to the total variance are plotted as o.

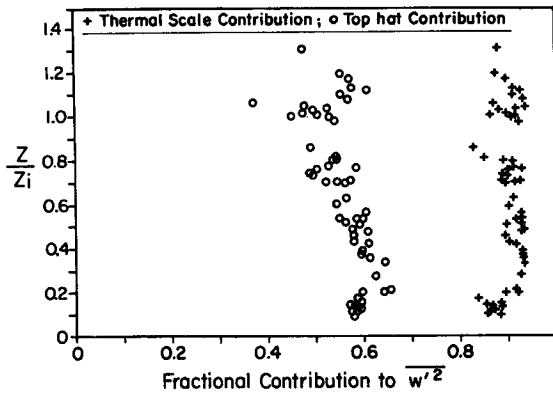


FIG. 6. As in Fig. 5 except for vertical velocity.

scales less than  $0.1z_i$  was much steeper in the stable air than in the CBL. Thus, in the inversion, a relatively larger portion of the variance is contributed by the thermal scales than by the smaller inertial subrange scales.

The profile of the top hat contribution to  $\theta_v$  variance is very different from that of the thermal scale contribution. The top hat contribution to the variance is an order of magnitude less than the thermal scale contribution in the lower CBL and up to two orders of magnitude less in the upper CBL. This same pattern can be found by computing the top hat contribution to temperature variance from the AMTEX results of Lenschow and Stephens (1980) and Lenschow et al. (1980). This upper CBL minimum in the ratio of the top hat contribution to the thermal scale contribution can occur only if the positive and negative thermal scale  $\theta_v$  perturbations are equally likely to be found in either thermal updrafts or in environmental downdrafts. This state was observed in the bivariate conditional sampling studies of Wilczak and Businger (1983) and Khalsa and Greenhut (1985b). The latter authors discuss the role of overturning updrafts in creating this situation.

Thus, while the  $\theta_v$  perturbations generated by entrainment across the capping inversion are on the same horizontal scale as the thermals they are not in phase with their primary updraft and downdraft structure. This observation can be understood in terms of the static stability profile of the CBL and capping inversion. In the unstably stratified lower CBL, buoyancy is a displacing force and, therefore, tends to be in phase with vertical motion. In the stably stratified regions of the upper CBL and capping inversion, buoyancy is a restoring force and, therefore, will tend to be 90 degrees out of phase with the vertical velocity. This same argument also explains the decrease with height of the correlation between  $w$  and buoyancy observed in Phoenix 78 and in previous observational, tank and LES studies (Deardorff, 1974a,b; Willis and Deardorff, 1974; Caughey and Palmer, 1979; Lenschow et al., 1980; Druilhet et al., 1983).

The top hat contribution and the thermal scale contribution to  $w$  variance for the individual flight legs are shown in Fig. 6. The thermal scale motions contribute 83% to 93% of the total variance throughout the CBL and capping inversion. This is similar to the fraction observed for  $\theta_v$  variance. The thermal scale contribution to vertical velocity variance is approximately constant with height because it depends directly upon the form of the  $w$  spectra which Kaimal et al. (1976) and Young (1987) have shown to vary little with height throughout the CBL.

The profile of the top hat contribution to the  $w$  variance is of similar form but has only two-thirds the magnitude of the thermal scale contribution. The AMTEX results of Lenschow and Stephens (1980) and Lenschow et al. (1980) show the top hat contribution to  $w$  variance decreasing with height. This difference could be related to their use of moisture to identify thermals if the correlation between moisture and  $w$  decreases with height as observed by Druilhet et al. (1983).

The top hat contribution and the thermal scale contribution to the covariance of  $w$  and  $\theta_v$  for the individual flight legs are shown in Fig. 7. The thermal scale motions contribute more than 95% of the total covariance in the lower CBL and more than 90% in the upper CBL. The thermals scale motions contribute a much larger fraction of the covariance than of the two variances. This difference is a result of the difference between the  $-5/3$  slopes of the  $w$  and  $\theta_v$  variance spectra in the inertial subrange and the  $-7/3$  or steeper slopes for the covariance spectra of  $w$  and  $\theta_v$  (Kaimal et al., 1972, 1976).

The top hat contribution to the covariance of  $w$  and  $\theta_v$  is approximately 60% of the total. This fraction is much greater than that for  $\theta_v$  variance but only slightly greater than that for  $w$  variance. Thus, top hat motions contribute significantly to the buoyancy flux in the upper CBL despite their negligible contribution to the buoyancy variance. The top hat contribution to the covariance for the individual flight legs do not cluster

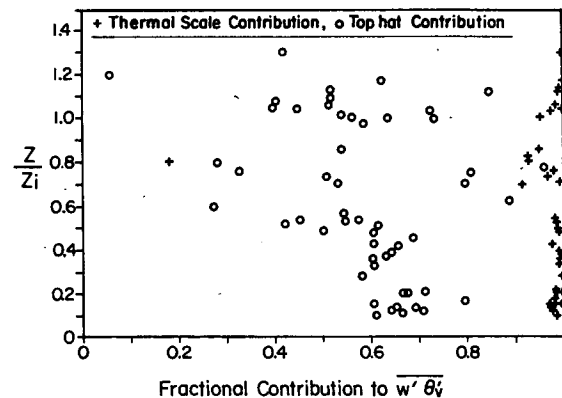


FIG. 7. As in Fig. 5 except for buoyancy flux.

as closely about a single profile as do the top hat contributions to the variances. Therefore, a top hat parameterization of the flux would have more uncertainty than a top hat parameterization of the variances.

#### 4. Conclusions

A conditional sampling technique for distinguishing thermal updrafts from environmental downdrafts has been developed. This technique removes the mesoscale and inertial subrange contributions to the turbulence from consideration when determining the boundaries between thermal updrafts and environmental downdrafts. Because the cutoff wavelengths of the low pass and high pass filters are defined with respect to  $z_i$ , they are located at the same two points in the spectra of  $w$  and temperature under the wide range of convective conditions under which those spectra are known to scale with  $z_i$ . Thus, if the results are sensitive to these cutoff wavelengths, this technique should yield more consistent results than previous techniques where width thresholds were a fixed number of meters and did not scale with  $z_i$ .

The width distributions of thermal updrafts and environmental downdrafts were observed to be approximately lognormal. However, the actual distributions could have been exponential because the filtering described above could theoretically modify such a distribution towards one indistinguishable from those observed. The updraft and downdraft width ranges which occupied most of the CBL area correspond to the wavelength of the peak of the vertical velocity spectra observed in the CBL.

The thermal updrafts were observed to be positively buoyant in the lower two thirds of the CBL and negatively buoyant in the upper third. The maximum in the profile of the mean vertical velocity in thermals occurred at one third of the CBL depth, only halfway up to the level of zero buoyancy. In addition, the observed  $w$  maximum was less than that which would result from free convection driven by the observed buoyancy profile. These two observations suggest that the lateral entrainment drag and/or pressure gradient forces are important in the vertical velocity budget of thermals.

The effects of the confinement of buoyant acceleration of thermal updrafts and environmental downdrafts to the lower two thirds of the CBL can be seen in the difference in the heights at which the maximum magnitude of these two flows occur. The buoyant acceleration of environmental downdrafts begins only after they have descended into the unstably stratified lower CBL while thermal updrafts experience buoyant acceleration only until they rise above the lower CBL. Therefore, downdrafts experience maximum net buoyant acceleration at the surface while updrafts experience it in the mid CBL. As a result, thermal updrafts reach their maximum magnitude at a higher level than do environmental downdrafts.

Thermal-scale motions contributed more than 80% to the variances of  $w$  and  $\theta_v$  and more than 90% of the covariance  $w$  and  $\theta_v$ . The contribution of thermal-scale motion to turbulence variances and covariance depends on the form of the variance and covariance spectra respectively. The  $\theta_v - w$  covariance spectra have steeper slopes in the inertial subrange than do the variance spectra of  $\theta_v$  and  $w$ . Therefore, thermal-scale motions account for a larger fraction of the  $\theta_v - w$  covariance than of the  $\theta_v$  and  $w$  variances. These results suggest that 80% or more of the turbulence variances and covariances are contributed by scales which are resolvable by LES models. These observations confirm the LES results of Moeng (1984) that buoyancy flux (or equivalently the buoyant production of turbulence kinetic energy) is almost completely resolvable by such a model.

The top hat contribution to the variances and covariance of  $w$  and  $\theta_v$  is much smaller than the thermal scale contribution. The top hat model of thermals and their environment fits the data best in the lower CBL where surface based buoyant convection dominates these statistics. In the upper CBL, the top hat model continues to account for a significant fraction of the variance of  $w$  and the covariance of  $\theta_v$  and  $w$  but contributes negligibly to the  $\theta_v$  variance. In this region, mixing of the stably stratified air is the primary source of  $\theta_v$  variance. The negligible contribution of the top hat model to  $\theta_v$  variance in the upper CBL suggests that while entrainment across the inversion produces variance on the thermal scales, it does not produce it in phase with the thermal plumes.

Observations of the top hat contribution to various turbulence statistics show that while the top hat model provides a useful description of the simpler bulk characteristics of thermals such as buoyancy and vertical velocity it is inappropriate for estimation of the higher order turbulence statistics of the CBL.

The observations in this paper and elsewhere suggest that there are qualitative differences in the structure of thermal updrafts and environmental downdrafts between the lower, unstably stratified, part of the CBL and the upper, stably stratified, part of the CBL. The primary indication of this difference is the decrease in magnitude of the correlation coefficient between  $\theta_v$  and  $w$  in the upper CBL. This decrease in correlation has been found for the total, top hat and thermal scale estimates. The observed difference in the phasing of buoyancy and vertical velocity perturbations between the lower CBL where buoyancy is a displacing force and the upper CBL where buoyancy is a restoring force matches that expected from simple theoretical parcel displacement arguments.

*Acknowledgments.* The author appreciates the assistance of the staff of the Research Aviation Facility of the National Center for Atmospheric Research in data acquisition. Discussions with P. H. Hildebrand, R. H.



Pielke were most helpful. I also  
 for typing the manuscript and Judy  
 the figures. The research reported  
 supported by the National Science  
 Grants ATM-8507961 and ATM-  
 the Office of Naval Research through  
 86-K-0688.

## REFERENCES

- and S. G. Palmer, 1979: Some aspects of turbulence through the depth of the convective boundary layer. *J. Roy. Meteor. Soc.*, **105**, 811-827.
- C. E., 1978: Boundary-layer evolution and nocturnal dispersal, Part II. *Bound.-Layer Meteor.*, **14**, 493-513.
- J. W., 1970: Convective velocity and temperature scales in the unstable planetary boundary layer and for Rayleigh convection. *J. Atmos. Sci.*, **27**, 1211-1213.
- 1974a: Three-dimensional numerical study of the height and mean structure of a heated planetary boundary layer. *Bound.-Layer Meteor.*, **7**, 81-106.
- 1974b: Three-dimensional numerical study of turbulence in an entraining mixed layer. *Bound.-Layer Meteor.*, **7**, 199-226.
- Jruilhet, A., J. P. Frangi, D. Guedalia and J. Fontan, 1983: Experimental studies of the turbulence structure parameters of the convective boundary layer. *J. Climate Appl. Meteor.*, **22**, 594-608.
- Greenhut, G. K., and S. J. S. Khalsa, 1982: Updraft and downdraft events in the atmospheric boundary layer over the equatorial Pacific Ocean. *J. Atmos. Sci.*, **39**, 1803-1818.
- Grossman, R. L., 1984: Bivariate conditional sampling of moisture flux over the tropical ocean. *J. Atmos. Sci.*, **41**, 3238-3253.
- Kaimal, J. C., Z. Izumi and O. R. Cote, 1972: Spectral characteristics of surface layer turbulence. *Quart. J. Roy. Meteor. Soc.*, **98**, 563-589.
- , J. C. Wyngaard, D. A. Haugen, O. R. Cote, Y. Izumi, S. J. Caughey and C. J. Readings, 1976: Turbulence structure in the convective boundary layer. *J. Atmos. Sci.*, **33**, 2152-2169.
- Khalsa, S. J. S., and G. K. Greenhut, 1985a: Conditional sampling of updrafts and downdrafts in the marine atmospheric boundary layer. *J. Atmos. Sci.*, **42**, 2550-2562.
- , and —, 1985b: Conditional sampling of penetrative updrafts and entraining downdrafts near the top of the marine atmospheric boundary layer. *Preprints Seventh Symp. on Turbulence and Diffusion*, Boulder, Amer. Meteor. Soc.
- Lamb, R. G., 1978: A numerical simulation of dispersion from an elevated point source in the convective planetary boundary layer. *Atmos. Environ.*, **12**, 1297-1304.
- Lenschow, D. H., and P. L. Stephens, 1980: The role of thermals in the convective boundary layer. *Bound.-Layer Meteor.*, **19**, 509-532.
- , and —, 1982: Mean vertical velocities and turbulence intensity inside and outside thermals. *Atmos. Environ.*, **16**, 761-764.
- , J. C. Wyngaard and W. T. Pennel, 1980: Mean-field and second moment budgets in a baroclinic, convective boundary layer. *J. Atmos. Sci.*, **31**, 465-474.
- Lopez, R. E., 1977: The lognormal distribution and cumulus cloud populations. *Mon. Wea. Rev.*, **105**, 869-872.
- Manton, M. J., 1977: On the structure of convection. *Bound.-Layer Meteor.*, **12**, 491-503.
- Melling, H., and R. List, 1980: Characteristics of vertical velocity fluctuations in a convective urban boundary layer. *J. Appl. Meteor.*, **19**, 1184-1195.
- Moeng, C.-H., 1984: A large-eddy-simulation model for the study of planetary boundary-layer turbulence. *J. Atmos. Sci.*, **41**, 2052-2062.
- Rayment, R., and C. J. Readings, 1974: A case study of the structure and energetics of an inversion. *Quart. J. Roy. Meteor. Soc.*, **100**, 221-223.
- Scorer, R. S., and F. H. Ludlam, 1953: Bubble theory of penetrative convection. *Quart. J. Roy. Meteor. Soc.*, **79**, 94-103.
- Taconet, O., and A. Weill, 1983: Convective plumes in the atmospheric boundary layer as observed with an acoustic Doppler sodar. *Bound.-Layer Meteor.*, **25**, 143-158.
- Wilczak, J. M., and J. A. Businger, 1983: Thermally indirect motions in the convective atmospheric boundary layer. *J. Atmos. Sci.*, **40**, 343-358.
- Willis, G. E., and J. W. Deardorff, 1974: A laboratory model of the unstable planetary boundary layer. *J. Atmos. Sci.*, **31**, 1297-1307.
- Wyngaard, J. C., and R. A. Brost, 1984: Top-down and bottom-up diffusion of a scalar in the convective boundary layer. *J. Atmos. Sci.*, **41**, 102-112.
- Young, G. S., 1987: Mixed layer spectra from aircraft measurements. *J. Atmos. Sci.*, **44**, 1251-1256.
- , 1988: Turbulence structure of the convective boundary layer. Part I: Variability of normalized turbulence statistics. *J. Atmos. Sci.*, **45**, 712-719.